

Uncertainties in azimuthal AVO analysis

Yong Xu*, Scott Pickford; Yongyi Li, Scott Pickford

Summary

As in conventional AVO analysis, uncertainties exist in azimuthal AVO analysis. Some uncertainties are discussed in this paper, including, reflection coefficient linear approximations, ambiguities to determine symmetry axis, weak anisotropy assumption, phase velocity vs group velocity, phase angle vs ray angle, and acquisition geometry irregularity. Errors and instabilities are focused on. Synthetic examples are designed to evaluate the uncertainties.

Introduction

Seismic detection of subsurface fractures has been found useful in fractured reservoir characterization. Horizontal transverse isotropy (HTI) model is commonly used in studies of fractured reservoirs that describes a system of parallel vertical penny-shaped cracks embedded in an isotropic host rock. Analysis of P wave reflection amplitude variation with offset and azimuth provides an approach to estimate anisotropic parameters in HTI media.

Ruger (1997) found that for HTI media, the anisotropic parameters (δ^0 , ε^0 , and γ after Thomsen, 1986, 1988) dominate the AVO gradient variation with azimuth. The anisotropic parameters (δ^0 , ε^0 , and γ) relate to crack density linearly (Bakulin, et al, 2000) in HTI media resulting from vertical fractures. Therefore, the information about the orientation, density, and content of vertical fractures (Bakulin, et al, 2000) is possible to be inverted from amplitude variation with offsets and azimuths. Azimuthal AVO (AVOZ) inversion and application has been studied by peer (Ruger 1997, Skoyles et al. 1999, etc.). As an extension of conventional AVO analysis with inclusion of azimuth dimension, AVOZ analysis is based on some approximations and assumptions. This paper explored how these factors cause the uncertainties in AVOZ analysis.

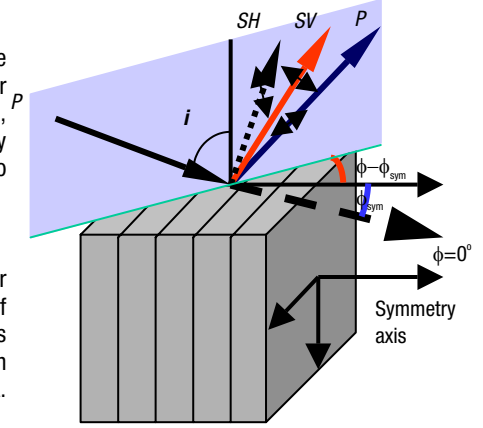


Figure 1. Illustration of an HTI model. The symmetry axis is perpendicular to fracture strikes.

Reflection coefficient with azimuth variation for HTI media

The reflection coefficients for HTI media are approximated as follow (Ruger, 1997):

$$R(i, \phi) = \frac{1}{2} \frac{\Delta Z}{Z} + \frac{1}{2} \left\{ \frac{\Delta \alpha}{\alpha} - \left(\frac{2\bar{\beta}}{\alpha} \right)^2 \frac{\Delta G}{G} + \left[\Delta \delta^{(V)} + 2 \left(\frac{2\bar{\beta}}{\alpha} \right)^2 \Delta \gamma \right] \cos^2 \phi \right\} \sin^2 i + \frac{1}{2} \left\{ \frac{\Delta \alpha}{\alpha} + \Delta \varepsilon^{(V)} \cos^4 \phi + \Delta \delta^{(V)} \sin^2 \phi \cos^2 \phi \right\} \sin^2 i \tan^2 i \quad (1)$$

where Z is P impedance, α and β are isotropic P and S velocities, and G is shear modulus.

The approximate reflection coefficient in equation (1) relates the AVO response to the anisotropy parameters and provide physical insight into the reflection amplitudes of P waves at boundaries of media with HTI symmetry. The magnitude of AVO gradient variation with azimuth is a function of the shear wave splitting parameter γ and the anisotropy parameter δ^0 related to P wave anisotropy. Equation (1) is valid for pre-critical incidence on an interface between two weakly anisotropic HTI media with the same symmetry-axis direction and small contrasts in the elastic properties across the boundary. As in Figure 1, the symmetry axis orientation might be defined as ϕ_{sym} because it is usually unknown in the real world. When incidence angle is small, the third term in equation (1) with $\sin^2 i \tan^2 i$ can be ignored and equation (1) is approximated to equation (2) in the following:

$$R(i, \phi) = A + B(\phi) \sin^2 i = A + \left[B^{iso} + B^{ani} \cos^2(\phi - \phi_{sym}) \right] \sin^2 i, \quad (2)$$

$$\text{where } A = \frac{1}{2} \frac{\Delta Z}{Z} = R_p, \quad B^{iso} = \frac{1}{2} \left[\frac{\Delta \alpha}{\alpha} - \left(\frac{2\bar{\beta}}{\alpha} \right)^2 \frac{\Delta G}{G} \right], \quad \text{and } B^{ani} = \frac{1}{2} \left[\Delta \delta^{(V)} + 2 \left(\frac{2\bar{\beta}}{\alpha} \right)^2 \Delta \gamma \right].$$

A more accurate expression for $R(i, \phi)$ than equation (2) without $\sin^2 i \tan^2 i$ term can be written as

$$R(i, \phi) = R_p (1 + \tan^2 i) - 2 \left(\frac{2\bar{\beta}}{\alpha} \right)^2 R_s \sin^2 i + B^{ani} \cos^2(\phi - \phi_{sym}) \sin^2 i, \quad (3)$$

$$\text{where } R_p = \frac{1}{2} \left(\frac{\Delta \alpha}{\alpha} + \frac{\Delta \rho}{\rho} \right) \quad \text{and} \quad R_s = \frac{1}{2} \left(\frac{\Delta \beta}{\beta} + \frac{\Delta \rho}{\rho} \right).$$

The accuracy of equations (1), (2), and (3) is compared in Figure 2 using two weak anisotropy models. Equation (3) more closely approximates equation (1) than equation (2) when incidence angle is larger than 25°.

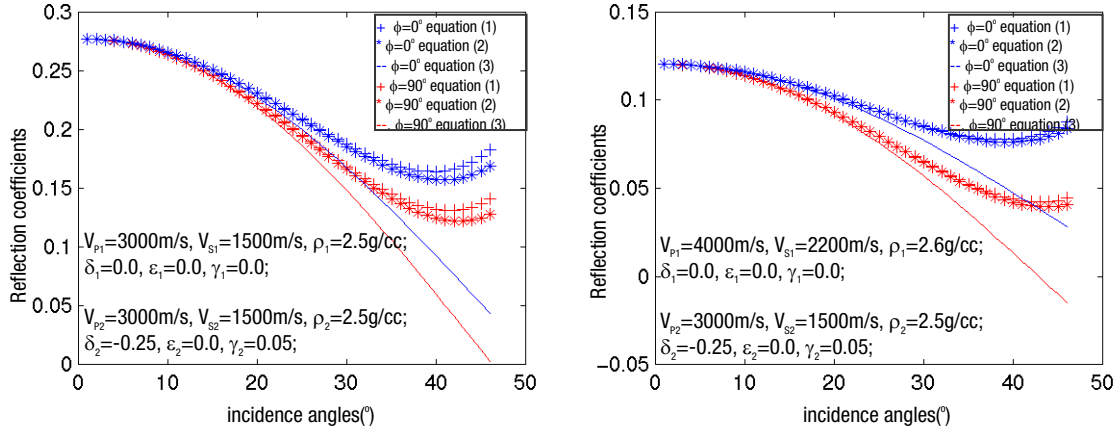


Figure 2. Comparisons of accuracy of three approximations of reflection coefficients at different incidence angles and azimuths parallel and perpendicular to symmetry axis ($\phi - \phi_{sym} = 0^\circ$ and 90°).

Inversion

In a 3D survey, reflection amplitudes are recorded at different offsets and azimuths and strong AVOZ is observed. The probable cause of AVOZ might be the presence of an orientated anisotropic medium. The simplest effective model of a formation containing a single fracture system is HTI medium. Based on the recent studies of HTI medium, it is possible to invert fracture orientation and density from AVOZ information. Approximations of reflection coefficient for HTI media, as equations (2) and (3), make it possible to do a generalized linear inversion, similar to conventional AVO inversion: when azimuths and incidence angles and reflection coefficients are known, A , B^{iso} , B^{ani} , and ϕ_{sym} can be inverted using equation (2) or R_p , R_s , B^{ani} , and ϕ_{sym} may be inverted using equation (3). However, the equations (2) and (3) are nonlinear with the unknown ϕ_{sym} . An approach suggested in published literature is separately solving ϕ_{sym} and other unknowns. The literature suggests that graphical interpretation be used to obtain the symmetry axis azimuth in the literatures (Ruger, 1997). Although graphical interpretation is a robust approach to determine the symmetry axis direction, More efficient approaches are needed to scan a large 3D data set with many samples and CDP locations. Using an automatic approach, the density and orientation of fractures are possible to be mapped and interpreted more efficiently.

In this paper, the ϕ_{sym} is solved using generalized linear inversion method to utilize the reflection amplitudes at all offsets and azimuths. Equation (2) is reformatted as a linear equation (equation (4)) with unknowns: C_{01} , C_{02} , C_1 , C_2 , and implicit ϕ_{sym} .

$$R = C_{01} + C_{02} \sin^2 i + C_1 \frac{1}{2} \cos(2\phi) \sin^2 i + \frac{1}{2} C_2 \sin(2\phi) \sin^2 i, \quad (4)$$

where $C_{01} = \frac{1}{2} \frac{\Delta Z}{Z}$, $C_{02} = B^{iso} + \frac{1}{2} B^{ani}$, $C_1 = B^{ani} \cos 2\phi_{sym}$, and $C_2 = B^{ani} \sin 2\phi_{sym}$.

Theoretically, C_{01} , C_{02} , C_1 , C_2 can be solved if at least four reflection amplitudes from different incidence angles and different azimuths are given. Consequently, the symmetry axis azimuth can be calculated using the solutions of C_1 and C_2 : $B^{ani} = \pm \sqrt{C_1^2 + C_2^2}$ and

$\phi_{sym} = \frac{1}{2} \arcsin \frac{C_2}{\sqrt{C_1^2 + C_2^2}}$, if $C_2 \geq 0$ or $\phi_{sym} = \pi + \frac{1}{2} \arcsin \frac{C_2}{\sqrt{C_1^2 + C_2^2}}$, if $C_2 < 0$. The solutions of symmetry axis azimuth

are non-unique due to two possible solutions of B^{ani} . *A priori* information is needed to find out the unique solution. According to the results of

Bakulin et al (2000), B^{ani} of HTI media resulting from fluid-filled vertical fractures with overlying isotropic media are non-negative, i.e.

$B^{ani} = \frac{16g}{3(3-2g)} e$, where $g = (Vs/Vp)^2$, and e is crack density. Usually g is smaller than 2/3. This observation throws lights on obtaining

unique solution of B^{ani} and ϕ_{sym} . Figure 3 is a diagram illustrating non-positive B^{ani} at a few possible situations. After symmetry axis azimuth is solved, more sophisticated inversion algorithms can be applied to solve other elastic parameters using equation (2) or (3), and other sophisticated corrections can be applied to reduce the biases of inversion.

As an example, a 3D CDP gather, that locates in the center of regular spacing square survey, is simulated to evaluate the inverse problem of equations (2), (3), and (4). Here, the condition number (ratio of maximum over minimum eigenvalues) of the linear system is evaluated as a criterion of stability, although condition number is not the only criterion. The condition numbers of the linear system from equations (2), (3), and (4) are plotted in Figure 4. Equation (4) has smaller condition number although it has four unknowns. The condition numbers for three equations have similar size. It is also observed that the exclusion of near zero incidences does not affect the condition number much, in other word, the far offset incidences dominate the solution stability. Examples show that the irregularity of acquisition geometry also affects the stability.

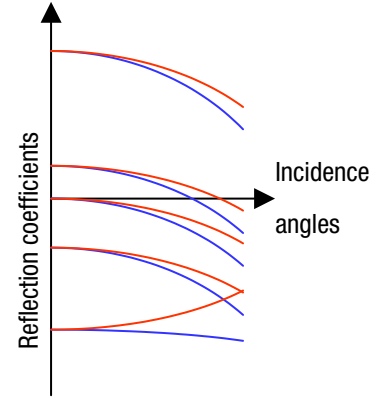


Figure 3. Diagram of reflection coefficients at the interface between isotropic media and HTI media resulting from fluid-filled vertical fractures: BLUE lines are for azimuth parallel to fracture strike; RED lines are for azimuth perpendicular to fracture strikes.

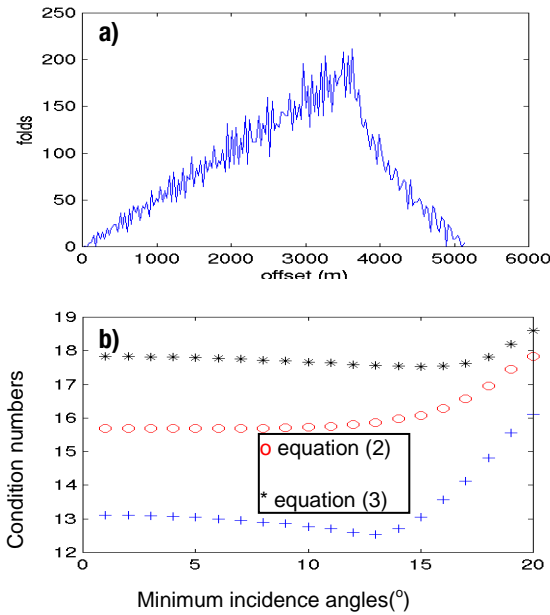


Figure 4. a) Fold distributions with offsets in the 3D CDP gather; b) condition numbers of inversions using equations (2), (3), and (4). In the tests of b), different incidence angle ranges are evaluated: the maximum angle is kept 36° , but the minimum angles are varying from 0° to 20° .

Using the model in Figure 4, noise-contaminated parameter inversions are tested for different RMS signal/noise ratios. Figure 5 shows the inversion results of such tests. It is observed that the solutions of R_p , and B^{ani} have similar accuracy using three equations at different noise/signal levels. The accuracy of inverted symmetry axis azimuth is affected by noise/signal ratios. Inverted azimuth error reaches 6° when RMS noise/signal ratio is equal to 4.

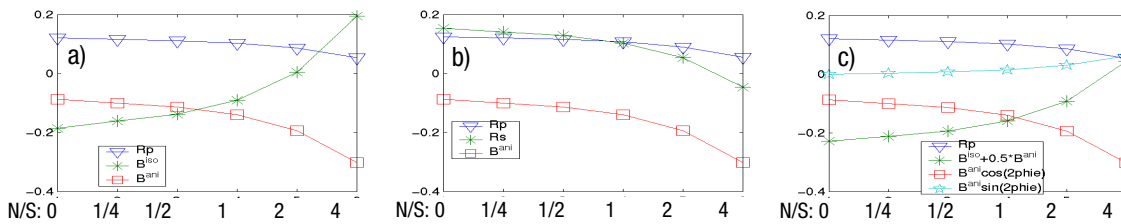


Figure 5. AVOZ inversion on a model based on equations (2), (3) and (4). Uniformly distributed random noise is added on the signal. From equation (4), the azimuth of symmetry axis is also solved. The solved azimuths of symmetry axis have larger error as noise levels increase:

RMS Noise/Signal ratio:	0	$\frac{1}{4}$	$\frac{1}{2}$	1	2	4
Solution of symmetry axis azimuth:	0°	1.1°	2°	3°	4.5°	6°

Limitations in AVOZ inversion:

The above discussions are based on some approximations and assumptions, which are more or less deviated from the reality. Equation (1) assumes weak anisotropy situation. The velocities in the above equations are phase velocities and the incidence angles are phase angles, while the energy a geophone recorded propagated at group velocity (strictly, energy velocity) and incidences at ray angles. However, the complexity of the problem and heavy computation make AVOZ inversion of energy reflections difficult. To use approximations based on equation (1) to do AVOZ inversion, phase velocity and group velocity, and, phase angle and ray angle have to be very close. Here, a few weakly anisotropic HTI models are designed to examine the deviations between phase and group velocities and between phase and ray angles. In Figure 6, phase and group velocities, phase and ray angles are compared for a few models. From Figure 6, it is noted that phase velocity and group velocity are close when ϵ is small. But the phase angles and ray angles might have large deviations (~5 degrees). These deviations might cause large biases on AVOZ inversion. Examples show that proper corrections can reduce these negative effects.

As in the above discussion, AVO gradient due to azimuth anisotropy (B^{azi}) is dominated by two anisotropic parameters: the shear-wave splitting parameter γ and coefficient δ . Studies (Bakulin, et al, 2000) show that for fractured fluid-filled cracks, γ and δ are linear to crack density. Therefore, crack density might remain the only anisotropic parameter to be inverted. However, the B^{azi} inverted from real seismic data can never be said to proportional to crack density due to the band-limited feature of seismic data and phase complexity. Scaling the inversion results to realistic crack density is thus being studied.

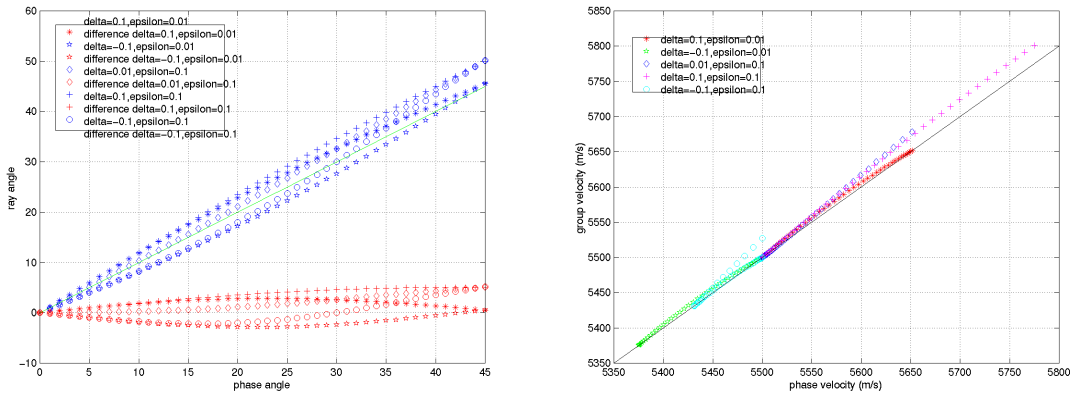


Figure 6. Comparisons between phase and ray angles and between phase and group velocities for different anisotropy parameter combinations.

Discussions

AVOZ inversion can be extended from conventional AVO inversion methodologies, however, inclusion of anisotropy and azimuthal dimension introduces uncertainties. Approximations and assumptions simplify the problem, but hurt the accuracy of inversion. Further studies are conducting to reduce the errors from the uncertainties.

References

Bakulin, A., Grechka, V., and Tsvinkin, I., 2000, Estimation of fracture parameters from reflection seismic data-part I, II, and III: Geophysics, Vol 65, No 6, 1788-1830.
 Ruger A., 1997, Variation of P-wave reflectivity with offset and azimuth in anisotropic media: Geophysics, Vol 63, No. 3, 935-947.
 Skoyles, D., et. al., 1999, Azimuthally dependent amplitude vs offset in 3D seismic: an automated statistical measurement and case study: Expanded Abstracts, 1999 SEG convention.
 Thomsen, L., 1986, Weak elastic anisotropy: Geophysics, Vol 51, No. 10, 1954-1966.
 Thomsen, L., 1988, Reflection seismology over azimuthally anisotropic media: Geophysics, Vol 53, No. 3, 304-313.